Direct Observation of the Phenomenology of a Solid Thermal Explosion Using Time-Resolved Proton Radiography

L. Smilowitz, B. F. Henson, J. J. Romero, B. W. Asay, C. L. Schwartz, A. Saunders, F. E. Merrill, C. L. Morris, K. Kwiatkowski, G. Hogan, P. Nedrow, M. M. Murray, T. N. Thompson, W. McNeil, P. Rightley, M. Marr-Lyon, and pRad Collaboration

Los Alamos National Laboratory, Los Alamos, New Mexico 87545

(Received 1 October 2007; published 4 June 2008)

We present a new phenomenology for burn propagation inside a thermal explosion based on dynamic radiography. Radiographic images were obtained of an aluminum cased solid cylindrical sample of a plastic bonded formulation of octahydro-1,3,5,7-tetranitro-1,3,5,7-tetrazocine. The phenomenology observed is ignition followed by cracking in the solid accompanied by the propagation of a radially symmetric front of increasing proton transmission. This is followed by a further increase in transmission through the sample, ending after approximately 100 μs. We show that these processes are consistent with the propagation of a convective burn front followed by consumption of the remaining solid by conductive particle burning.

DOI: 10.1103/PhysRevLett.100.228301 PACS numbers: 82.33.Vx, 25.40.Cm, 82.30.Lp, 82.40.−g

Compared to supersonic detonation phenomena, the subsonic release of energy in solid thermal explosions is only primitively understood on a fundamental level for any energetic material. HMX (octahydro-1,3,5,7-tetranitro-1,3,5,7-tetrazocine) is a powerful energetic nitramine explosive used in a variety of applications. Considerable laboratory [1–6] and modeling work [7–10] have been devoted to one-dimensional linear burning in HMX formulations. However, attempts to implement this understanding into simulations have had to settle for external, integral observations of explosive response [11–14], and proceed without any direct observation of the phenomenology of divergent, three-dimensional burning subsequent to internal thermal ignition of a solid explosive [15,16]. In this Letter we report the first direct observation of burn propagation inside a thermal explosion of PBX 9501. The application of the Proton Radiography (pRad) facility at Los Alamos National Laboratory, yields proton transmission images within a solid thermal explosion. With these data we identify both convective and conductive burning mechanisms subsequent to thermal ignition within the solid and measure the rates of these processes during a thermal explosion for the first time. Using synchronized proton images with few μs interframe time during the explosion, we initially observed spatially heterogeneous patterns in the images, which we attribute to cracking in the explosive, accompanied by a radially symmetric structure in the proton transmission emanating from the ignition volume. We further observed consumption of the solid explosive, as well as the deformation and destruction of the metal case, over approximately 100 μs. By inference of solid mass from proton transmission we calculate the evolution of solid density loss and infer a mechanism of internal burning during the explosion.

While the rate of energy release in a thermal explosion may accelerate even into the supersonic detonation regime, it begins with a very nonlinear thermal ignition, wherein chemical energy is released, and temperature increased, with a rate that depends on temperature. This nonlinear temporal evolution and acceleration of the process has precluded the synchronization of a thermal explosion with any modern, fast radiographic method with sufficient timing accuracy to enable imaging of the density of the energetic material within the explosion. This is in contrast to detonation, where prompt shock initiation has enabled the application of x-ray and proton radiographic techniques for decades. We have recently reported a new technique for synchronizing the timing of a thermal ignition while preserving the inherent features in the subsequent evolution of the explosion [17]. By application of a laser pulse to directly illuminate the hottest volume of material during thermal runaway, the so-called ignition volume, we accelerate the thermal ignition and induce explosion within 100 μs. This is sufficiently fast in the thermal explosion regime to enable radiography of a thermal explosion.

The sample consisted of two right circular cylinders of PBX 9501 12.7 mm in diameter by 12.7 mm in height joined along the cylinder axis to form a single 2 to 1 aspect ratio cylinder encased in aluminum 3.2 mm thick. The two halves define a midplane in the sample where thermocouples and a 200 μm core optical fiber were introduced [see Fig. 1(b)]. The assembled halves were glued at the case to seal the sample, and the end caps were compressed by external bolts anchored in the end caps as shown in Fig. 1(a). We used the 1064 nm fundamental wavelength of a pulsed Nd:YAG laser as the heat pulse which synchronized ignition to the accelerator. The laser was operated in free running mode, delivering approximately 50 mJ in 150 μs. The laser pulse was coupled into the 200 μm optical fiber that was delivered through the aluminum case and ended approximately 1 mm from the center of the sample.

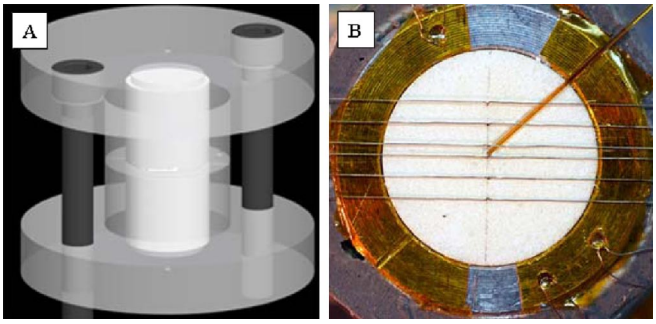

FIG. 1 (color online). (a) Schematic drawing of the solid cylindrical experiment. The PBX 9501 sample is shown in white and the aluminum case in gray. The sample midplane can be seen as the plane bisecting the two cylinders. (b) Picture of the midplane of one sample during construction. The aluminum case and white PBX 9501 are shown with the thermocouples and fiber optic in place on the midplane.

Transmission images were obtained using 800 MeV proton radiography at Los Alamos National Laboratory [18]. The magnification in these experiments gives a full field of view in the object plane of 46×46 mm with a spatial resolution of ~ 100 μm [19]. Both absolute transmission and change in transmission images were used in the analysis. The gray scale indicates the transmission intensity which is related to areal density. Proton transmission was converted to areal density using a transmission model based on measured proton-target nuclear interactions and multiple Coulomb scattering.

Four images from a single experiment, viewed transverse to the cylinder axis (the side view), are shown in Fig. 2. The images were obtained at 26, 40, 54, and 61 μs after ignition, defined as the central temperature rise [17]. The vertical lines along the case are the nichrome heating wires used to heat the sample. The opening of the midplane and early leaking of product gases is evident in the first image. The motion of the case wall as the experiment opens is seen in the subsequent images, beginning approximately 45 μs after ignition. Four additional images, viewed along the cylinder axis (radial view) and obtained from a different experiment, are shown in Fig. 3. The images were obtained at 9, 16, 37, and 51 μs after ignition. The images are characterized by (i) the early formation of a heterogeneous pattern of dark lines (increased transmission), which increase in contrast and complexity throughout Figs. 3(a)–3(d), (ii) a circular boundary, darkening and increasing in width throughout, which is the motion of the aluminum case boundary in response to pressure, and (iii) a radially symmetric darkening of the field throughout, which will be discussed below and is consistent with the decrease of solid explosive density. These observations have been reproduced with three experiments imaged in this configuration at two magnifications.

The first details observed subsequent to ignition involve the spatially heterogeneous patterns which develop in the transmission images which we interpret as the formation of

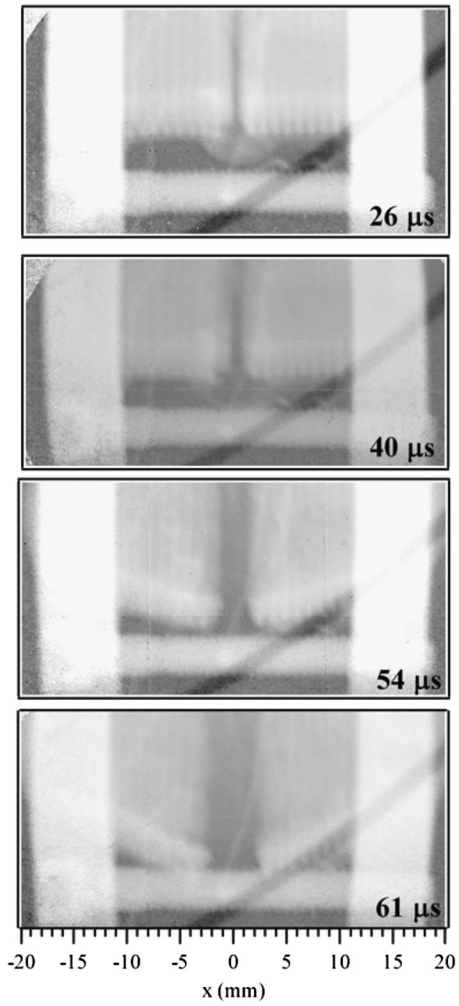

FIG. 2. Four images taken with the side view from a single experiment. The gray scale is constant for all frames and is the proton transmission, with light corresponding to low transmission. The image time was measured relative to the central thermocouple trigger.

a network of cracks throughout the volume of the solid, emanating from the ignition volume. This phenomena has been observed previously in experiments designed to enable the optical viewing of a two-dimensional sample at ignition [20]. Early pressurization of the assembly is sufficient to place the solid in tension due to internal pressurization and, as the material maintains some strength at these temperatures, this leads to cracking. This observation is the first verification of this mechanism internal to a three-dimensional explosion.

A radially symmetric increase in proton transmission (decrease in density) can also be seen, superimposed on the crack pattern, from numerical analysis of the images. This is shown in Fig. 4 where the radial transmission intensity is plotted as a function of diameter in the radial view, starting 2 μs from ignition. These curves have been averaged azimuthally over 180°, such that each curve is a radial average over half of the cylinder, negative diameter representing one half and positive the other. These aver-

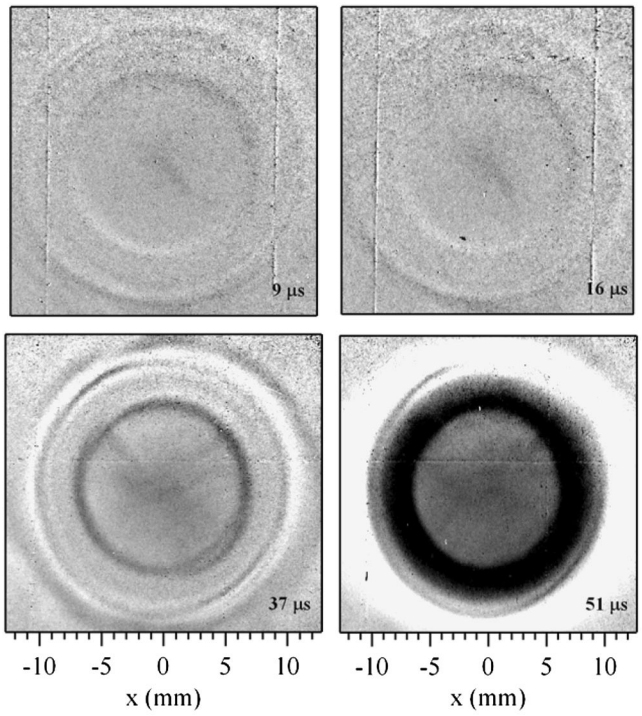

FIG. 3. Images taken in the radial view from a single experiment. The gray scale is the change in proton transmission normalized to a static image, with dark corresponding to high change in transmission. The image time was measured relative to the central thermocouple trigger.

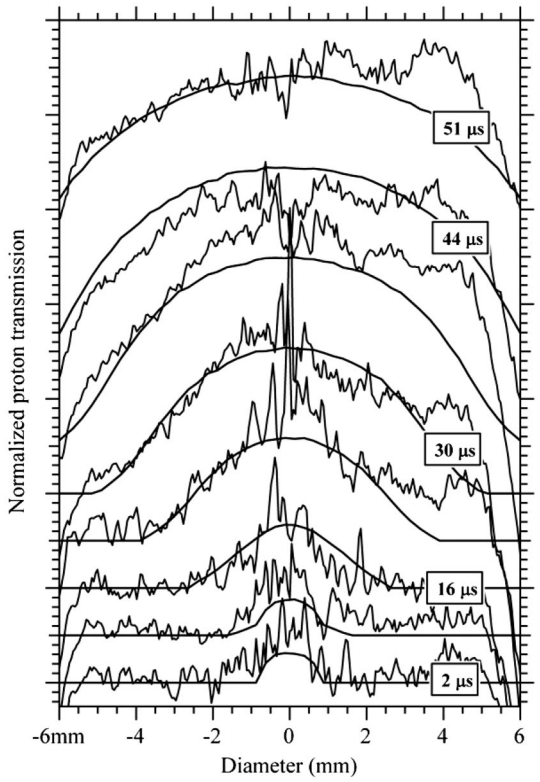

FIG. 4. Proton transmission recorded along a diameter in the radial view. The data are normalized to 1 for transmission through the initial solid explosive and vertically offset. Data from 13 images are shown in 7 μs intervals starting at 2 μs subsequent to ignition. The solid lines are calculations of normalized density using a model of convective propagation of ignition and consumption by conductive burning.

ages have been taken using several arbitrary planes bisecting the cylinder, all with similar results. The symmetry is somewhat more evident in the negative diameter half of the cylinder using this bisecting plane but is nevertheless robust. The curves have also been normalized to 1 in the transmission through the explosive.

At early times, from 2 to 9 μs, a relatively static volume of low density is observed in the center of the field, corresponding to the ignition volume. At approximately 16 μs the boundary of the radially symmetric feature begins to expand, and transmission within the feature increases. The boundaries of this feature reach the cylinder wall position 6.7 mm from the central ignition at approximately 37 μs. At this time, the increase in transmission becomes less radially distinct and by 51 μs appears relatively flat across the field. The side view images of Fig. 2 show intact cylinder wall position as late as 40 μs, indicating that the decrease in solid density in the radial view of Fig. 3 is not due to flow of solid material.

One interpretation of this radially symmetric structure is the propagation of a convective burn front by gas phase permeation through the material, followed by the loss of solid by conductive burning. This suggests a mechanism based on one-dimensional convective [2] and conductive [5] burning in HMX. In this mechanism of internal, spherically divergent burning, a propagating convective front ignites the solid, which is then consumed by a conductive burn. An important assumption in this model is that the convective front emanates radially from the ignition volume, and is either independent of the crack network formed previously or based upon a finer, spatially isotropic network structure unresolved in these images.

We have developed a model with which to calculate the loss of solid to burning using a simple Monte Carlo (MC) simulation of the combined convective ignition or conductive consumption mechanism. Figure 4 illustrates some example calculations as solid black lines through the transmission data extracted from the images. At the time corresponding to each curve in Fig. 4 the density along the line integral through the sample is calculated as a function of diameter. The model assumes radial symmetry (either spherical or elliptical) about the center point of the cylinder and a plane of symmetry bisecting the cylinder at the instrumented midplane. The MC routine samples points along the 12.7 mm line of site through one half of the cylinder at points along the diameter. Points lying outside the location of the convective front at that time are assigned a progress variable of zero. Points lying within a volume about the center assumed to be consumed by ignition are assigned a progress variable of 1. For points between these limits the conductive burn time is calculated as the time from passage of the convective front. For such a point on

the diameter, x, and a point along the cylinder length, y, this is given by

$$t = \frac{R - \sqrt{(x^2 + y^2)(1 - \{\varepsilon \cos[\arctan(y/x)]\}^2)}}{v}, \quad (1)$$

where t is the time since passage of the convective front, v is the radial velocity of the convective front, and R is the current radius of the convective front. To allow for the possibility of a faster convective rate along the axial direction, ε is an elliptical eccentricity equal to $\sqrt{1 - (\alpha)^2}$, where α is the ratio of the radial over the axial velocities. The extent of consumption is calculated from a sigmoidal function, based on this time, as $p = 1/(1 + e^{-(t-6.0)/3.0})$, where p is a progress variable spanning 0 to 1 over approximately 20 μs and proportional to density. The sum of values at each MC step, 0 for material ahead of convection, 0 to 1 in the volume, and 1 for completely consumed, is integrated and normalized, yielding a density normalized to 1 at full density. We assume this to be equivalent to the normalized transmission in Fig. 4.

This simulation uses (i) a fixed radial velocity, which is directly observed in the data as the diameter where transmission begins to increase in each frame, (ii) the possibility of higher axial velocities due to increased confinement away from the release at the midplane, and (iii) a description, in the form of the sigmoidal rate parameters, of the progress of consumption by conductive burning. The calculations of Fig. 4 were based on the measured radial velocity of 165 m/s and a spherically emanating convective front with $\varepsilon = 1$. The sigmoidal function itself is consistent with a nucleation and growth type conductive burn, and the half time of 6.0 μs used here can be coupled with an assumed conductive velocity to give a length scale for the coalescence of independent burn fronts. The parameters used here also indicate a nonzero progress at zero time, $p(0) = 0.12$, which may be interpreted as that solid fraction consumed by the convective burn front. Further simulations are underway to parametrize variables such as ε and the half time of conductive consumption.

Good agreement with the data is obtained from this simulation, particularly on the negative side of the cylinder. Variations on the positive side may reflect real perturbations to symmetry that arise from the cracking pattern upon which the convective front is superimposed. Classical convective [2] and conductive [5] burning are driven by gas phase pressurization, typically parametrized as a power law in the linear regression rate as a function of pressure [2]. From Ref. [2] a pressure of 868 MPa would be required to drive the measured convective velocity of 165 m/s. Assuming the conductive rate is driven by the same pressure, the conductive burning data [5] yield a conductive rate of 0.86 m/s and a length scale for conductive burning of 10 μm in these experiments.

In conclusion, we provide the first direct observations of burn propagation in a thermal explosion. The proton transmission images give a quantitative measure of the evolution of solid density in a thermal explosion. They confirm the macroscopic cracking of solid explosive as an early response to pressurization in the explosion followed by convective ignition and conductive consumption of material. We measure the rate of convective burning in the radial direction and from these data have begun to construct models of burning and consumption taken directly from observation. These models can be incorporated into larger scale simulations of high explosive systems response.

The authors acknowledge the support and direction of Dr. Philip Howe in initiating this work. This research was supported by Science Campaign 2 and the Surety Program administered by Los Alamos National Laboratory, as well as the Joint Munitions Program administered by both the Departments of Energy and Defense.

[1] A. I. Atwood, T. L. Boggs, P. O. Curran, T. P. Parr, D. M. Hanson-Parr, C. F. Price, and J. Wiknich, J. Propul. Power **15**, 740 (1999).
[2] T. L. Boggs, Prog. Astronaut. Aeronaut. **90**, 121 (1984).
[3] M. Herrmann, W. Engel, and N. Eisenreich, Propellants Explos. Pyrotech. **17**, 190 (1992).
[4] N. Kubota, J. Propul. Power **15**, 759 (1999).
[5] J. L. Maienschein, J. F. Wardell, M. R. DeHaven, and C. K. Black, Propellants Explos. Pyrotech. **29**, 287 (2004).
[6] A. Zenin, J. Propul. Power **11**, 752 (1995).
[7] Y. C. Liau and J. L. Lyman, Combust. Sci. Technol. **174**, 141 (2002).
[8] K. Prasad, R. A. Yetter, and M. D. Smooke, Combust. Flame **115**, 406 (1998).
[9] M. J. Ward, S. F. Son, and M. Q. Brewster, Combust. Theory Modell. **2**, 293 (1998).
[10] E. B. Washburn and M. W. Beckstead, J. Propul. Power **22**, 938 (2006).
[11] S. K. Chidester, C. M. Tarver, L. G. Green, and P. A. Urtiew, Combust. Flame **110**, 264 (1997).
[12] F. Garcia, K. S. Vandersall, J. W. Forbes, C. M. Tarver, and D. Greenwood, AIP Conf. Proc. **706**, 947 (2004).
[13] F. Garcia, K. S. Vandersall, J. W. Forbes, C. M. Tarver, and D. Greenwood, AIP Conf. Proc. **845**, 1061 (2006).
[14] M. J. Kaneshige, A. M. Renlund, R. G. Schmitt, and W. W. Erikson, AIP Conf. Proc. **706**, 351 (2004).
[15] M. D. Cook and P. J. Haskins, AIP Conf. Proc. **429**, 337 (1998).
[16] J. J. Yoh, M. A. McClelland, J. L. Maienschein, A. L. Nichols, and C. M. Tarver, J. Appl. Phys. **100**, 073515 (2006).
[17] L. Smilowitz, B. F. Henson, M. M. Sandstrom, J. J. Romero, and B. W. Asay, Appl. Phys. Lett. **90**, 244102 (2007).
[18] C. T. Mottershead and J. D. Zumbro, in *Proceedings of the IEEE Particle Accelerator Conference, Vancouver, Canada*(IEEE, Piscataway, NJ, 1998), pp. 1397.
[19] C. Morris, J. W. Hopson, and P. Goldstone, Los Alamos Sci. **32**, 32 (2006).
[20] P. M. Dickson, B. W. Asay, B. F. Henson, and L. B. Smilowitz, Proc. R. Soc. A **460**, 3447 (2004).